Evaluation of consolidation of grout injection with ultrasonic tomography

Fernando Jorne *, Fernando M.A. Henriques, Luis G. Baltazar

UNIC, Department of Civil Engineering, Universidade Nova de Lisboa, Campus da Caparica, 2829-516 Caparica, Portugal
*Corresponding author. Tel.: +351 21 2948580; fax: +351 21 2948398
E-mail addresses: fjorne@fct.unl.pt (Fernando Jorne)

Abstract

Old masonries especially in the case of multi-leaf walls often present low compactness and very few links between the internal and external leaves. The injection of grouts in the core of the multi-leaf masonries is one of the techniques used most frequently for consolidation. In order to test the effectiveness of the filling process and the bonding of the grout to the masonry materials, ultrasonic tomography was conducted complemented with mechanical tests. The mechanical results showed good correlation with ultrasonic results and density gradients along the porous medium injected were obtained. Moreover, it was confirmed the importance of the bond properties of the interfaces (grout - porous medium particles) on the mechanical results. Regarding the ultrasonic tomography, the research demonstrated a correspondence between the characteristics of the porous media after the injection and the information displayed in the tomographs. Thus, it is proved that ultrasonic tomography is a useful technique to evaluate effectiveness of the grout injections, allowing an understanding of the ability of the injections to modify the physical and mechanical properties of an injected porous medium. This research has special relevance due to lack of information about the study of grout injection capacity in physical models (simulating the old masonries), through tomography and mechanical tests when compared to the amount of information that already exists in the case of study of grout injectability tests.

KEYWORDS: Grout injection technique, old masonries, hydraulic lime grouts, grout injection tests, mechanical tests, contact angle test, ultrasonic tomography

1 Introduction

The space between the two external leaves in multi-leaf wall is typically filled with loose, low-strength material made of small pieces of stones and/or bricks and mortar. Due to the weak connections between outer leaves, the predominantly irregular morphology of the walls, the presence of voids and the low strength of the mortar used, three-leaf masonries are very vulnerable to in-plane (mainly shear) and out-of-plane actions [1]. To enhance the compactness of the interior weak leaf, as well as to re-instate the links between external and internal leaves in three leaf masonry, the technique of grouting is often applied [2]. In this way, the "effectiveness of grout injection" can be defined as the ability of the grout to fill the voids and to establish the bonding between the materials of the wall after hardening, which consequently improves mechanical properties [3]. In other words, the idea behind the concept of grout is to use a material with high injectability and bonding properties. An ideal grout will increase the cohesion of the historic masonry and through its own adhesion to it, yielding enhanced mechanical behavior of the system as a whole [4].

Given the irreversibility of injection grouting, attention needs to focus on the selection of injection grouts which are compatible with the in situ materials. The current tendency is to use grouts that respect compatibility physically and chemically with masonry materials, such as hydraulic lime grouts [5-7]. As expected, such grout mixes exhibit reduced mechanical properties as compared to the cement based mixes. Nevertheless, previous research [6] has proven that repair materials with high mechanical properties are not as efficient as expected in terms of strength enhancement of historic grouted masonry. Furthermore, several authors [1,8-9] found that the compressive strength of grout injected walls (i.e. the increase in this strength after grouting) was not directly proportional to the compressive strength of the injection grouts used for grouting. In turn, as previously mentioned, an important parameter for the improvement of the behaviour of stone masonry strengthened by grout injection is the bond between grout and the in situ material, which is not necessarily proportional to the compressive or tensile strength of the grout. The bond mechanism between different porous media (PM in the present work) and grouts was also studied by Adami and Vintzileou [10], who performed shear tests, as well as direct tension tests. The results obtained showed the important influence of the substrate characteristics (i.e. the surface roughness, porosity, and initial water content) on the bond properties. In order to study the above parameters, an experimental program was designed composed mainly of two phases: (i) in the fresh state, grout injection tests in reduced models (cylinders) were made to evaluate the injectability of the grout in different porous media (ii) in the hardened state, the cylinders that resulted from injection tests were evaluated through non-destructive techniques (NDTs) and mechanical tests.

In what concerns the mechanical tests, splitting tests were performed to different injected porous media. This study aims to contribute to a better understanding of the prevailing mode of failure and the influence of the type of material, distribution of voids size and water content of the particles (at the time of injection) in the mechanical bonds at the interfaces (grout - PM). Furthermore, it is also analysed the strength gradient along the height of the cylinder, as well as the relation with the effectiveness of grout injection technique for each PM.

Among the various NDTs, acoustic techniques, based on measurements of the characteristics of acoustic waves propagating through the material, appear to be of great usefulness since they are non-invasive, easy to use and provide relevant information about internal morphology of the injected material [11]. Thus, they are often used in laboratory for materials characterisation and structural diagnosis [12-13]. Acoustic analysis is based on a simple principle of physics: the propagation of any wave will be affected by the medium through which it travels. Thereby, changes in measurable parameters associated with the passage of a wave through a material can be correlated with changes in the physical properties of the material [1-2,14]. Thus, in the present work, ultrasonic tomography was used to evaluate the effectiveness of grout injection techniques for the strengthening of multi-leaf stone masonry walls, since it is possible to obtain a qualitative information about the compactness of the PM from the outputs of ultrasonic tomography [15]. In this way, the locations in which injection is more difficult to penetrate (areas of masonry consisting of solid stones or a mixture of different particles which prevent the injection of grout) can be detected [1,16]. To this end, a comparative tomography of porous media after injection was carried out. The tomographs were obtained with specific software, in the present case 3DTOM and GeoTom CG. The software take as input a data set of travel-time measurements and compute a three-dimensional model of velocity in the material containing the ray paths [14,17]. The SIRT (Simultaneous Iteration Reconstruction Technique) iterative method was implemented to solve the system in both programs in order to easily obtain a map of the wave velocity distribution in the tomographic section.

The tomographic analysis also allowed establishing a relation with mechanical results. From the tomographs it was also possible to identify different density gradients along the height of the cylinder, since there is a relation between the velocity of the ultrasound and the compactness of the media [18-19]. Being so, this research has special relevance due to lack of information about the study of grout injection capacity in physical models filled with different porous media (simulating old masonries), through tomography and mechanical tests, when compared to the amount of information that already exists for injectability tests [5,20-24]. The results summarised in this paper are part of a larger study where the performance of the grout injection technique (in fresh and hardened state) is analysed in different porous media that simulate old masonry walls.

2 Material studied

2.1 The mechanism bond

Research conducted by several authors [6] indicated that the bond between grout and PM is of both chemical (because of the reactions between the materials in contact along the interfaces) and (mainly) mechanical. Mechanical bond depends on characteristics of the substratum, such as density, surface porosity and pore size, roughness, water content and water absorption capacity. Thus, it is extremely important to know the values of these properties for the different PM studied. In addition, it also depends on the properties of the binding material, in particular its chemical composition, fineness, setting time and expansibility phenomena.

2.2 Porous media properties

In order to study the grout injection capacity, injectability tests were made. Given the difficulties to reproduce a historical masonry due to their high heterogeneity [23] and to the difficulty of reproducing the characteristics of ancient grouts [25-26], old masonries were simulated using simplified models which were built by combining three different crushed limestone sands and three different crushed bricks (Fig. 1). The same method but with different materials was used in works of other authors [20,23-24]. The materials were washed, dried and sieved to obtain diverse grain size distributions to enable the simulation of different permeabilities of masonries. Five different grain size media types were adopted to simulate different masonries (Fig. 2).

Fig. 1- Three different grain size ranges (coarse, medium, fine). Limestone sand (above) and crushed brick (below)

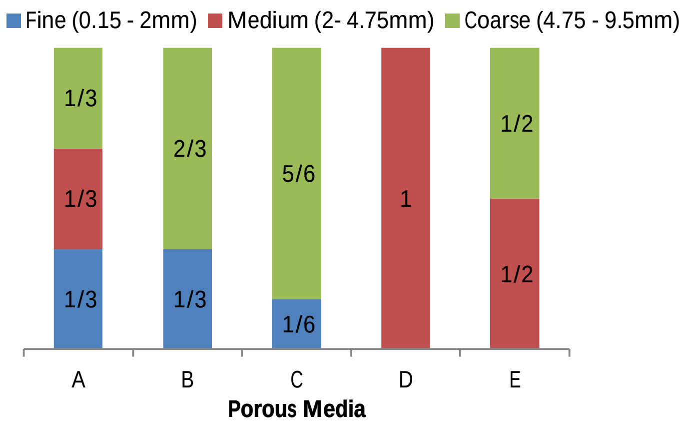

Fig. 2 - Different grain size ranges of the porous media studied

In accordance with the survey of the sections of multi-leaves masonry done by certain authors [25,27] some parameters were adopted (Table 1) to characterize the different PM, namely: the parameter d(90) and d(10), respectively the diameter through which 90% and 10% of the total mass passes.

The total porosity of each PM type was evaluated by measuring the volume of water which could be filled inside each cylinder (Table 1). The range values obtained are between 40-55%, which is a typical range of percentages in research of masonry walls, if only the dimensions of the inner core are computed [23]. It is worth to note that this parameter does not give the value of porosity that the grout can penetrate inside the PM, which in fact is much smaller, since the volume accessible depends on the fluid behaviour. In fact, the solid particles of the grout suspension (Bingham fluid) cannot enter all of the voids as can a Newtonian fluid [21,28].

Table 1 - Porous media characteristics

	Porous media type									
	A		B		C		D		E	
	stone	*Brick*	*stone*	*Brick*	*stone*	*Brick*	*stone*	*Brick*	*stone*	*Brick*
d(90) [mm]	8.17	8.22	8.97	8.82	9.00	8.97	4.58	4.50	8.62	8.59
d(10) [mm]	0.60	0.34	0.58	0.32	1.08	0.67	2.41	2.17	2.66	2.38
P.M. porosity [%]	41.2	48.1	39.3	48.7	44.6	51.5	50.4	56.6	48.4	55.4
WA (%)	5.6	19.4	3.9	19.1	2.2	16.2	2.2	14.3	1.5	12.5
Specific Surface (mm^2/mm^3)	5,03	6,06	4,90	5,84	3,17	3,38	2,86	2,63	2,02	1,72

To study the water absorption capacity and porous structure of the particles of each porous medium, the cumulative pore size distribution was evaluated using the mercury intrusion porosimetry (MIP) with an AutoPore IV 9500 mercury porosimeter. The brick and limestone samples were dried in an oven at 105^0C before testing. Cylindrical pore geometry and a contact angle of 140^0 were assumed [29]. From the graphic presented in Fig. 3 (each curve is the average of three tests) it can be observed in both samples the inexistence of a pore diameter to which the highest slope of mercury injection (threshold diameter [30]) corresponds.
However, the curvature of cumulative pore size distribution of limestone is more pronounced, which indicates a narrow distribution of the pores. Indeed, the main pore diameter is significantly larger in brick (0.015 - 4.5 µm) than for the limestone samples (0.025 - 0.045 µm). Moreover, the area below the cumulative intrusion curve is much higher in brick samples. Thereby, it is possible to state that brick samples, with higher porosity and pores size, have higher water absorption capacity when water or grout is being injected. These results fit well with the water absorption (WA) capacity of each PM (Table 1) calculated by the European standard EN 1097-6. The knowledge of water absorption capacity of the particles of PM is of utmost importance during the injection of grouts [20,24]. This allows a perception of the amount of water absorbed by the particles of PM during the injection process, which influences the grout fluidity (consequently the grout injection capacity) and the mechanical bond between the grout - PM particles, since the water that is absorbed by the surface particles of PM forces the binder grains to stick to its walls creating an interfacial layer (grout - PM particle) with high binder content which provides a better bond between both. Thus, on one hand, brick PM create more resistance to the grout flow and, on the other hand, establishes a greater bond with the grout.

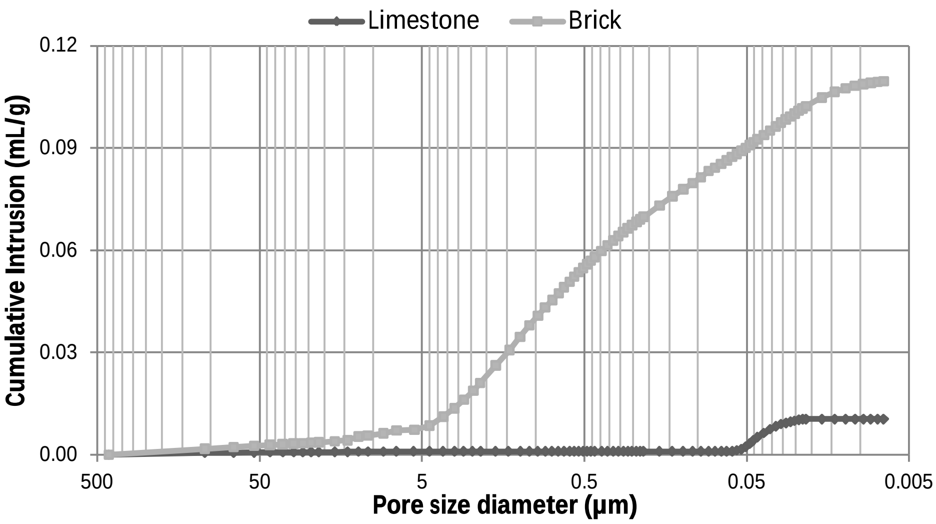

Fig. 3 - Cumulative pore size distribution to brick and limestone samples

Another output from (MIP) is the bulk density [31]. The results of density are also in consonance with porosity, because the former increases while the latter decreases, as expected. In fact, stone particles with lower porosity have higher bulk density (3,60 g/cm^3) than brick particles (2,00 g/cm^3).

The grout wettability quantifies the wettability of a solid surface by a grout. For the same grout, wettability depends on the type of surface in terms of water absorption capacity and roughness [32]. Therefore it is possible to conclude that the grout wettability is directly related to the bond between grout and PM particle, meaning that when a grout has high wettability the bond with PM is generally also high. In this work, the grout wettability was characterized by contact angle measurements. The contact angle is a quantitative measure of the solid angle (θ) of a fluid on a given surface [33], determined in this work with a sessile drop apparatus (Goniometer KSV instruments) using porous medium particles (which are polar as most construction materials).

A high contact angle (θ) indicates a grout with low affinity for the polar surface (poor wetting). This means that a lower contact angle is desirable to get a grout with higher wettability and, as a result, with greater bond. But, on the other hand, the grout wettability is directly related with the grout retention capability and it can also be seen as an indicator of its fluidity, because high water loss (high wettability) is a drawback in grout flow capacity [34]. Thus, in what concerns the evaluation of the effectiveness of grout injection it should be taken into account that the contact angle has an opposite trend for the grout fluidity and the bond strength between grout and the porous media particles. Table 2 shows the contact angles of grouts with different PM. As seen, the contact angle is higher in stone particle surface and when PM particle is wetted. The results show a considerable variation which means a significant alteration on grout wettability.

Table 2 - Contact angle (Θ) between grout and particle surface of PM

PM		Contact angle - Θ (º)
Stone	Dry	48
	Wetted	76
brick	Dry	35
	Wetted	54

2.3 Grout design

2.3.1 Grout composition

Grout design involves the study of the behaviour of a suspension in fresh and hardened state. The required performances of grout at the fresh state are: high penetrability, stability of the suspension and limited or no bleeding [35]. These characteristics may be affected by many parameters, namely the type of binder, the water/binder ratio, the type and percentage of superplasticizer and the mixing procedure. The used binder was NHL5 hydraulic lime (EN459-1) produced in Portugal by Secil-Martingança with a water/binder ratio (w/b) of 50% in weight. According to the bibliography and particularly following the recommendations proposed by Valluzzi [23], a minimum value of water/binder = 55% (in weight) should be used; in the present study only 50% was used due to the presence of the superplasticizer (Glenium Sky 617 with a dosage of 1.2% in weight) which causes a significant increase in the fluidity of the grout [5,36].

2.3.2 Mixing procedures

The hydraulic lime mixes were prepared at room temperature 22±1.5°C and 53% of relative humidity. For the preparation of grouts ordinary tap water was used and dry hydraulic lime was hand mixed to ensure a homogeneous distribution before the beginning of the mechanic mixing. The mixing procedure was chosen in accordance with previous research of Baltazar *et al* [37].

3 Procedure

3.1 Injection Tests

In order to study the grout injection capacity simplified models were used to analyse the penetration of the grout in the masonry [23,25]. The models were prepared with transparent Plexiglas cylinders with diameter 144 mm and height 300 mm, as in ASTM C943. They were filled with one of the media types trying to reproduce as much as possible real situations, such as the inner core of a multi-leaf masonry.

For injection purposes a device based on previous works [20,21,24,38] was used (Fig. 4). The filled cylinders were injected with the fresh natural hydraulic lime grouts immediately after grout preparation. The injections were performed at constant pressure of 1 bar from the bottom to the top [20,23].

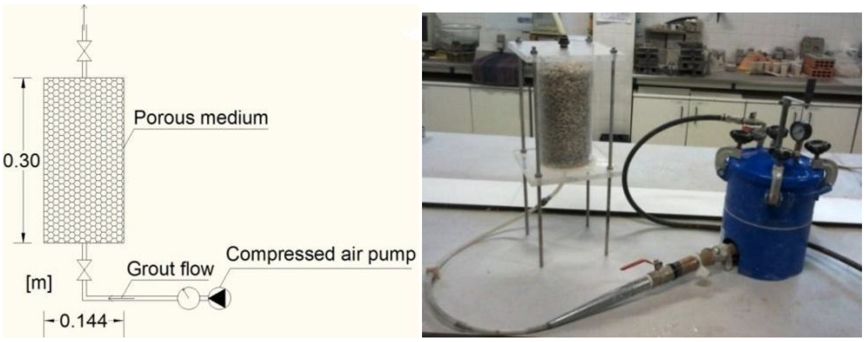

Fig. 4 - Setup for injection tests used in lab

3.1.1 Porous media with different moisture content

Since it is not expected masonries to be always dry, the media of some cylinders were pre-wetted by simple injection with water (in accordance with experiments of Valluzzi [23], Van Rickstal [24] and Anzani [39]. After the injection of water the valve at the bottom of the cylinder was opened to allow the water to flow out of the sample. Half an hour later the same sample was injected with the hydraulic lime grout. Injection tests for the five media types were done with and without pre-wetting of the porous media in order to evaluate the effect of the water content of porous media on the injectability of the grout and posteriorly in mechanical properties of the injected cylinders.

3.2 Mechanical properties

In the first part of this article it was mentioned that the mechanical properties of the grout are not much relevant since pure grout will not be present in the injected masonry. Instead it is more useful to test the mechanical strength of the injected cylinder samples. For this purpose cylinders were kept in normal laboratory conditions for 45 days (T=20ºC and R.H.=65%) after the injection. The characterization of the mechanical properties was carried out only for the samples in which the grout reached the top of the cylinder (PM types C, D and E).

The Plexiglas cylinders were removed from the hardened samples and the ultrasound pulse velocity was measured in order to obtain the tomographs (Fig. 5). After that the cylinders were cut in 3 slices and each of these slices was also analysed for ultrasound pulse velocity and the tensile splitting strength was determined.

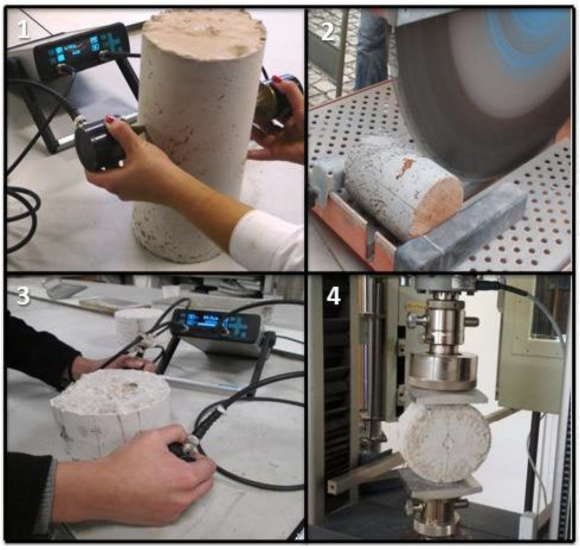

Fig. 5 - 1) Ultrasound pulse velocity test (for a cylinder); 2) slice of the cylinder; 3) and 4) ultrasound pulse velocity and splitting test, respectively (for a slice of cylinder)

3.2.1 Splitting tests

The indirect tensile strength test was carried out according with ASTM C 496 test procedure. This test consists on applying a compressive force along the length of a cylindrical specimen at a prescribed rate until failure occurs (Fig. 5). This load induces tensile stresses on the plane perpendicular to the load. The test is considered valid only if the failure occurs along the load direction in the middle of the specimen.

The tensile strength is calculated at the theoretical failure section where the tensile stress is maximum:

$$T = \frac{2P}{\pi \times l \times d} \tag{1}$$

where T is the splitting tensile strength (MPa), P the maximum applied load indicated by the testing machine (N), l the length (mm), and d is the diameter (mm).

The diameter of the samples is 144 mm and the height 80 mm, a value that is lower than the prescription of the standard. This reduced height was required to allow the evaluation of the effectiveness of the injection at three different levels.

Making a parallelism with the old masonries, the results of tensile splitting tests of cylinders (which represent the inner core of the strengthened masonry wall) can be used to estimate the ability of grout to improve the tensile strength of ancient masonry walls with this type of pore size distribution [1].

3.2.2 Ultrasonic pulse velocity tests

The ultrasonic technique is based on the generation of ultrasonic impulses at a selected point of the sample. Based on the time (measured by a pundit equipment) that the impulse takes to cover the distance between the transmitter and the receiver, the overall quality and homogeneity of the tested cylinder can be assessed [1,40-41]. In general terms, more compacted materials with higher density will have high wave propagation velocities. Instead, air interfaces (or voids) within a cylinder will cause variations in the pulse velocity, since the wave pulse is forced to circumvent the internal air void, the time of propagation for the assumed path through the void centre is increased, causing in this way, the decrease of the apparent velocity. Thus, air interfaces are registered as places with very low wave propagation velocity [42].

The choice of appropriate frequency depends on the type of the evaluated material, since the attenuation magnitude of the ultrasonic waves (that varies according to the heterogeneity degree of the material) is dependent on the value of selected frequency [2]. The present work used 54 kHz ultrasonic transducers that are able to locate small anomalies (such as minor flaws/voids) [46], which is especially important in the case of small laboratory samples. Low frequency pulse tests limit the identification of smaller flaws and voids due to the higher energy and resistance to attenuation in the presence of multiple cracks and flaws, what may not be critical when testing in situ real masonries.

The ultrasonic tests were aimed at controlling the effectiveness of the injection by evaluating the compactness at different heights [14,16]. Thus, the measurements were performed in the middle of each slice corresponding to the three levels (bottom, middle and top) of each cylinder (Fig. 5). To obtain the average ultrasonic velocity of each slice to detect the penetration and diffusion of the grout, a system of measuring points, i.e., a grid pattern, was established (Fig. 6). The grid refinement is dependent on the: sample size, variability expected and the accuracy required [11].

Since the degree of saturation of the samples affects ultrasonic pulse velocity [43], all samples were dried prior to be tested.

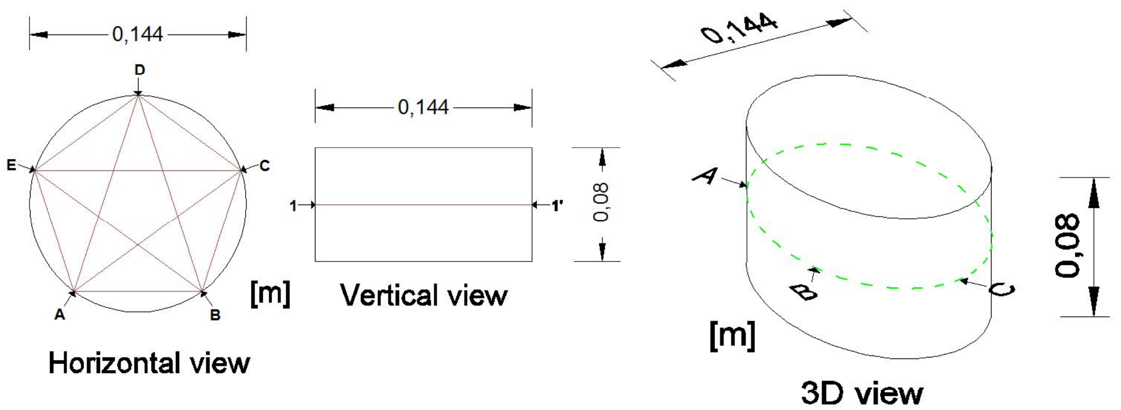

Fig. 6 - Scheme of the mesh grid used to measure the average ultrasonic velocity for each slice of the cylinders

3.2.3 Ultrasonic tomography

The ultrasonic techniques are preferentially carried out applying the direct transmission because it is very effective, since the broad direction of wave propagation is perpendicular to the source surface and the signal travels through the entire thickness of the sample. However, the direct transmission has some limits as well. The major limit consists in describing the wave's characteristics of the sample using for each path only one value of that characteristic, i.e., hypothesising that the mean value is homogeneous along each wave path. This assumption prevents the identification of the position of the detected anomaly inside the sample/cylinder. An effective way to overcome this limit is to use tomography which allows the reconstruction of an image of the inside of the cylinder [44]. The tomographic imaging is a computational technique (GEOTOM CG and 3DTOM are the software used) that utilizes an iterative method (SIRT algorithm) for processing a large quantity of data (ultrasonic pulse velocities) collected on the external surface to reproduce the morphological internal structure of a sample [11,16,45]. The final output is a map of the velocity distribution on a plane section of the structure under investigation, which allows the evaluation of the effectiveness of repair technique [46-48].

The section of the cylinder investigated was marked by a mesh grid (Fig. 7) whose dimension was related to the expected resolution and to the distance between two subsequent transmission or receiving points [11].

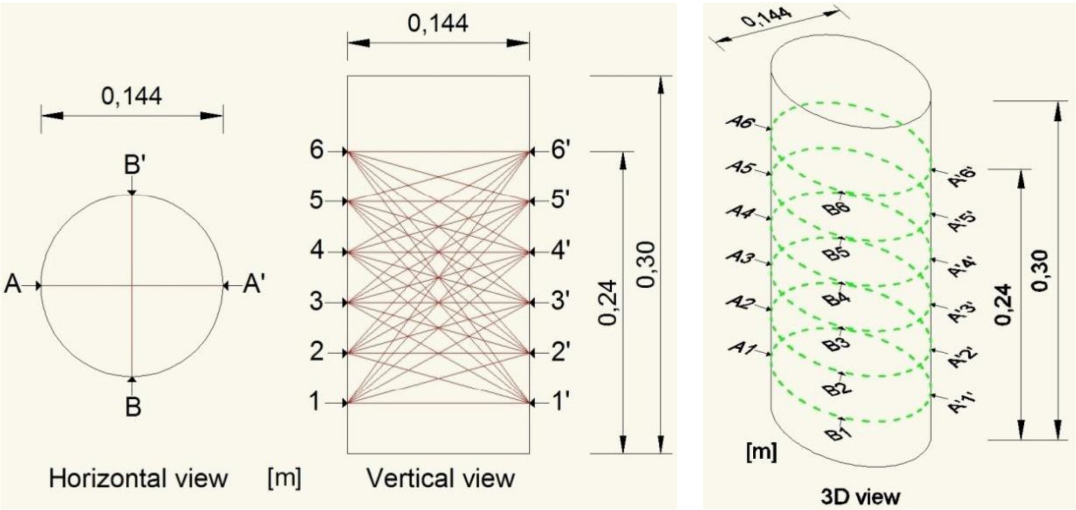

Fig. 7 - Scheme of the mesh grid to obtain ultrasonic tomographs along the height of the cylinder

4 Results and discussion

The characterization of the mechanical properties of the samples (in which the grout injection reaches the top of the injection) was done with direct ultrasonic measurements, splitting tests and ultrasonic tomography.

4.1 Visual inspections after injection of the cylindrical models

After 45 days the cylinders were cut and an inspection of the degree of success of the injection in terms of penetration and diffusion of the grout was possible. A remark can be made regarding the presence of large amount of not injected zones for porous media with finer material, as shown in Fig. 8 - a). In contrast, when PM do not have any presence of finer particles, a high effectiveness of grout injection is achieved (Fig. 8 - b-c)).

Fig. 8 - Porous media C (left), D (middle) and E (right picture). The core in the left picture displays a big void

4.2 Splitting test

Splitting tests enable the determination of grout bond to the porous media injected. Only a grout with good behaviour will improve the load bearing capacity of masonry [27]. The splitting tensile strength values are reported in Table 3. It can be remarked that the strength values are ranging from 0.18 to 0.40 MPa for limestone PM and from 0.24 to 0.62 MPa for crushed brick PM depending on the effectiveness of injection. These results fit well with similar results reported in the literature [49]. Samples C showed a lower strength (both for crushed brick and limestone), probably because of the lower porosity and the lower aperture of the voids of porous media (Table 1) before injection (causing phenomena of filtration and blockages to the grout flow) induces lower amounts of injected material (Table 5) [25,50], i.e., lower effectiveness of grout injection capacity (Fig. 8 and Fig. 14).

From Table 3, it is obvious that the mechanical results highly depend on the position of the specimen in the original sample. For some samples (cylinders) the relation between mechanical strength show a positive gradient (i.e. increase of the strength values along the height of the cylinder) whereas for other there is a negative gradient. Two phenomena can cause a density gradient. While the grout is going up through the cylinder filled with PM particles, its W/C ratio decreases because the particles absorb some of the water. This water absorption leads to an increase of the density of the grout also contributing to an increase of its cohesion resulting in a positive gradient strength (Table 3). But it happens only if the PM is dry at the time of injection. On the contrary, when PM is pre-wetted before the injection the w/b ratio is higher (because the grout does not lose so much water to the PM) which causes an increase of free water amount that contributes to increase shrinkage and instability phenomena - segregation and bleeding [5, 51]. Shrinkage is one of the most important problems in what concerns injections; according to the work of Toumbakari [9] a relatively low shrinkage is required for a good bond. In relation to the instability phenomena, the separation of liquid phase of grout (water) and solid phase (binder) will increase, yielding a difference in binder concentration that can occur vertically (especially for higher heights) due to gravitational settling of the binder grains, as shown in Fig. 9. This causes a strength gradient in the injected zone: a stronger zone downwards because of a higher binder concentration and a weaker zone on top. This negative strength gradient is clearly noticeable when analyzing the strength results (Table 3). This observation shows that the maximum injection height is not only limited by the hydrostatic pressure, but also by the strength gradient which arises in cases like this [24].

Fig. 9 - Cylinder $C_{stone,,wetted}$ (left picture) and $C_{brick,wetted}$ (right picture) 45 days after of the injection time

In the case of PM C the density gradient is negative in both situations. The resistance of the fine voids to the flow increases at greater distance from the injection hole. Due to this increasing resistance finally the yield stress will not be reached at the front of the injection [24]. This blocking mechanism produces a slow obstruction of the injection. When the grout loses too much water the viscosity and the yield stress become too high to make any further penetration possible. This phenomenon is more visible when PM have fine particles, which is the case of PM C (Fig. 14).

Table 3 - Splitting tensile strength [MPa] for different cylinder parts (bottom, middle and top) of porous media C, D and E

Splitting Tensile Strength [MPa]		Limestone					Crushed *Brick*				
Porous Medium		bottom	middle	top	**Average**	Gradient [MPa/m]	bottom	middle	top	**Average**	Gradient [MPa/m]
C	*dry*	0,28	0,24	0,22	**0,24**	-0,38	0.41	0.21	0.11	**0.24**	-1,88
	wetted	0,25	0,20	0,10	**0,18**	-0,94	0.38	0.21	0.13	**0.24**	-1,56
D	*dry*	0,25	0,28	0,30	**0,28**	0,31	0.47	0.56	0.58	**0.54**	0,69
	wetted	0,25	0,22	0,15	**0,21**	-0,63	0.54	0.52	0.54	**0.54**	0,00
E	*dry*	0,33	0,40	0,47	**0,40**	0,88	0.54	0.62	0.72	**0.62**	1,13
	wetted	0,33	0,31	0,18	**0,27**	-0,94	0.62	0.62	0.56	**0.60**	-0,38

According to the results of Vintzileou [6] the prevailing mode of failure in the tensile splitting test was the bond between the PM particles and the grout, regardless of the type of material analysed. In all PM, higher values (by 75% approximately) of the splitting tensile strength were obtained for brick PM when compared with the limestone PM (Table 3). This is attributed to the better mechanical adhesion achieved of the interface grout-brick particles consequence of its higher grout wettability (higher grout affinity with the particle polar surface as shown in contact angle results - Table 2) [6,8], which promotes the emergence of important chemical reactions in the contact area between particles surface and the grout paste during the hydration process. In case of limestone particles (non-porous aggregates), there is no release of ions from particles surface susceptible of combining with ions derived from the hydrated grout. Thus, the binding will only be established by simple deposition of constituents of grout hydrated, i.e., physical connections.

Comparing the splitting tensile results of various cylinders (Table 3), it is possible to observe that for both materials PM E has the highest results. Since the prevailing mode of failure in splitting test is through the bond between grout and PM particles, for PM without relevant voids such as PM D and E the one with lower number of interfaces (Fig. 8) will have the higher mechanical results, which in this case is PM E.

The water content of the interfacial zone is another parameter with extreme relevance on the bond between the grout and the PM particles. As PM particles are completely embedded in the grout, they absorb the water of the grout which provides a better adhesion between both. By injecting water the masonry will be saturated and, although the grout will pass easier (since it is more fluid), the contact angle between grout and particles surface will be higher (poor wetting, meaning poor bond). Furthermore, the W/C ratio of the grout after injection will remain very high, producing a weaker binding material in the hardened state. The little absorption needed for a good adhesion between grout and masonry does not occur and the mechanical improvements will be poor [5,23-24]. Thus, it is possible to state that although pre-wetting can improve the penetration of the grout inside the masonry, it has deleterious effects on mechanical strength, strength gradient and stability of the injected grout.

4.3 Ultrasonic velocity test

The measurement of pulse ultrasonic velocity by transmission in a material is a relatively simple and fast test, as explained previously. From Table 4 it is possible to observe a velocity variation in function of the height above the injection point, i.e., there is a velocity gradient depending on the height of injection. Since there is a relation between the velocity of the ultrasound and compactness and density of the media [18-19], the presence of density gradients can be inferred. The gradient is negative in the case of injections of wet porous media and positive when the porous media is dry at the time of injection. In the case of dry porous media one phenomenon can explain the positive density gradient. While the grout is going up through the cylinder its w/b ratio decreases because the PM absorb some of the water, which lead to an increase of the density of the grout. This phenomenon was also reported by Van Rickstal [52]. The only exception is $C_{,brick,dry}$ (Table 4) due to the obstruction created by dry finer particles to the grout flux along the height of injection, as shown in Fig. 14.

Comparing the gradient trend of ultrasonic velocity (Table 4) and splitting tensile strength (Table 3), it is possible to observe that there exists a great coherence. Thus, when ultrasonic tests showed a significant variance of the velocity along the height of the cylinder, it is possible to conclude that the mechanical characteristics follow the same trend. PM C is an example of this, as shown in Table 3 and Table 4.

Table 4 - Vertical distribution of the Ultrasonic velocity (m/s) measured in different cylinder parts (bottom, middle and top)

Ultrasonic velocity (m/s)		**Limestone**					**Crushed Brick**				
Porous Medium		bottom	middle	top	**Average**	**Gradient**	bottom	middle	top	**Average**	**Gradient**
C	*dry*	1839	1994	2066	**1966**	+	1924	1890	1581	**1799**	-
	wetted	1896	1655	1644	**1732**	-	1663	1508	1474	**1548**	-
D	*dry*	1920	2021	2079	**2040**	+	1869	1873	1949	**1897**	+
	wetted	2124	2087	1874	**2028**	-	2027	1978	1987	**1997**	-
E	*dry*	2352	2409	2472	**2444**	+	1825	1841	1878	**1881**	+
	wetted	2337	2335	2108	**2260**	-	2123	2098	2036	**2086**	-

From Table 4 it can be seen that for each limestone porous media the velocity values of pre-wetted samples were lower, due to the higher amount of free water after the grout injection. As a result, after hardening it is observed a larger number of voids in the cylinder which attenuates the ultrasonic waves. Indeed, the voids in the interior of cylinders act to scatter some of the initial energy of the compressional wave pulse away from the original wave path. Such results fit well with similar results obtained by Anzani [39], Panzera [41] and Naik [42]. In fact, after pre-wetting of PM not all the injected water flow away, so for the same PM the grout mass injected in wetted PM is smaller than in dry PM, as shown in Table 5. After the injection process the dry PM does not have any presence of free water. In contrast, in pre-wetted porous media free water is present which means that during the curing process when the water evaporates, some voids within the porous media are left.

According to Panzera [41] and Anzani [2], for heterogeneous materials such as the PM studied in this work, ultrasonic velocity value depends not only on porosity but also on attenuation due to dispersion at the internal interfaces porous media particles–grout. Since when a propagating wave pulse impinges on an interface, a portion of the wave energy is scattered away from the original wave path (i.e., dissipation of energy occurs). Thus, as shown in Table 4, for coarser PM (D and E) without relevant voids after injection, the PM D with more interfaces present lower values of ultrasonic velocity.

Regarding the brick PM, from Table 4 it is clear that pre-wetting can solve penetrability problems (the obstruction to grout injection is reduced), since the average ultrasonic velocities are higher for PM wetted. On the other hand, since there is no water absorption out of the grout, the mechanical strength of these particular samples is very poor, as shown in splitting test results (Table 3). Therefore, as already stated by Van Rickstal, pre-wetting has to be used with caution [24].

Table 5 - Grout mass injected for the different PM used [kg]

Porous Media		*Grout mass injected [kg]*	
		Stone	*Brick OB*
C	dry	*3.92*	*3.62*
	wetted	3.30	3.24
D	dry	4.51	4.76
	wetted	3.95	3.80
E	dry	*4.41*	*4.33*
	wetted	3.98	3.89

Given the results obtained, it is possible to state that the direct ultrasonic tests can be used to improve the injection technique and to control the penetration and diffusion of the grout during the works in laboratory. This conclusion is in accordance with the results of some authors as Anzani [39] and Da Porto [15].

4.4 Relation among experimental tests results that characterise the grout injection

Some of the results shown previously were combined and analysed together with the radar graph of Fig. 10, in which the average of the results for different PM are represented in percentage (100% being the highest value for each test result). From this graph some general relations already reported can be observed, namely the relation between the amount of injected grout (in mass) with the ultrasonic velocities (US) and between the results of splitting tensile strength (ST) and the inverse of contact angle (1/θ). Concerning the first relation, it is clear that the higher the presence of grout in a PM (i.e., a better quality of injection), the greater is the measured ultrasonic velocity since there are less voids. Regarding the second relation, it is observed that higher 1/θ values correspond to higher splitting tensile strengths due to the stronger bonds between grout and the particle surface of PM. Taking into account the splitting test results displayed in Fig. 10, the bond strength between grout and PM particles has greater importance than the percentage of voids filled with the grout, i.e., the mass of injected grout for each porous medium (Table 5). Actually, limestone PM exhibited lower splitting tensile strength values than brick PM, in spite of the similar injectabilities of grout in either PM.

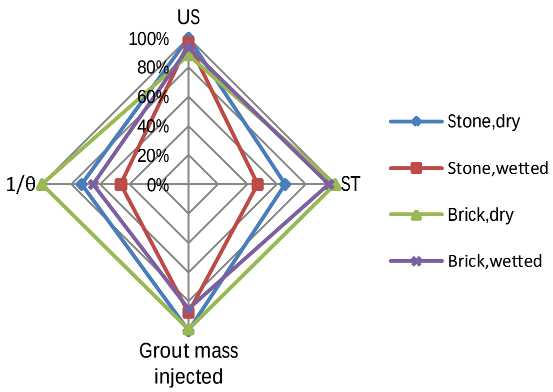

Fig. 10 - Relation among experimental tests results that characterise the grout injection

4.5 Ultrasonic tomography

4.5.1 Methods and algorithms

Data inversion was performed through the SIRT iterative method. The technique yielded the velocity field in the cross section of the sample. Another technique established to perform ultrasonic tomography of a sample is the RAYPT (Ray-projection technique), a constrained optimization technique designed for imaging discrete anomalies in a uniform background material, which it is not the case of cylinders studied and for this reason was not used. The calculations with SIRT are based on a three-dimensional rectilinear grid of node points, with intervening volume elements or voxels. Values of velocity are specified at the nodes, and calculated within voxels by multiple linear interpolation. Furthermore, in an imperfectly elastic material, intrinsic attenuation causes an exponential decay of wave amplitude with distance from the point source, since the waves lose some energy due to internal friction (depending on the magnitude of the loss of the physical properties of the medium) [17,45]. Thus, it is worthwhile to note that the tight grid of measurements used allowed defining more precisely the shape of the voids, thus achieving a sharper resolution, with the drawback of implying longer measuring and computational times. This observation fits well with the results obtained by Concu [44,47] and Cantini [11]**.** This last author noticed the influence of the density of the ray path map (that depends directly on the mesh grid chosen), highlighting the benefit of some redundancy for a better resolution of the tomographs; this allows a noise reduction in the velocity map and a better detection of the local inhomogeneities.

In 3DTOM calculations as ray tracing and travel-time computation may be carried out in several ways, ranging from fast and approximate to time-consuming and accurate. The straight-ray approximation allows very rapid calculation of model travel times, but its validity diminishes with large velocity contrasts. So, given the heterogeneity of the samples studied, this method was not chosen. Curved-ray calculations involve a great deal more of computation, but are more accurate for strong contrasts. There are three methods: "ray-bending", "network theory" and a hybrid approach that uses both the network and ray-bending methods which causes longer execution times, but is the most accurate of the approachs available [17], since it can solve the main problems associated with other methods. For this reason, this was the chosen method. As regards ray-bending, the problem is that the calculations may converge to a local minimum rather than a global minimum time path. However, this problem is solved through the use of network method where all paths correspond to global minimum travel time (which means first-arrival paths). The problem of network method is that the paths are rather angular and appear "unphysical", but they can be iteratively improved by the bending algorithm [17].

4.5.2 Ultrasonic Tomographs

In this section the ultrasonic tomographs will be compared with the photos that were taken during the inspection tests of the cylinders and with the mechanical results presented in 4.2. Ultrasonic tomographs of horizontal sections for each level (bottom, middle and top) of the ultrasonic grid (Fig. 6) were obtained. These ultrasonic velocities are influenced by local voids along their paths, thus the results reported for each level can indicate significant differences depending on the area and location of voids present.

Some results from cylinders characterized by the presence of fine material are worthy of attention. It is the case of porous media $C_{stone,dry}$ it shows low velocities in zones that before the injection presented finer PM material. This trend is systematically observed on the cylinders filled with this specific porous medium, resulting in a non-homogeneous state after injection. Regarding the tomographs, in case of the medium slice (Fig. 11 - left), more voids are concentrated in the core (characterized by the lowest values of ultrasonic velocity ranging between 850-1300 m/s). Related to the borders, the high velocities (from 2000 to 2500 m/s) indicate good compactness. These results are consistent with the inspections conducted on cylinders after being cut in slices, as shown in Fig. 11 - left below. The top slice of cylinder $C_{stone,dry}$ is shown in Fig. 11 – right, showing a two layer pattern with a higher velocity at the compact region of the cylinder and lower velocity in two zones where there are two voids: a large on the right side and a small one in bottom left side of the sample, as shown in Fig. 11 - right below. In this way, some of the ray-paths of the horizontal tomographies crossed these voids, which attenuate the ultrasonic waves in these areas.

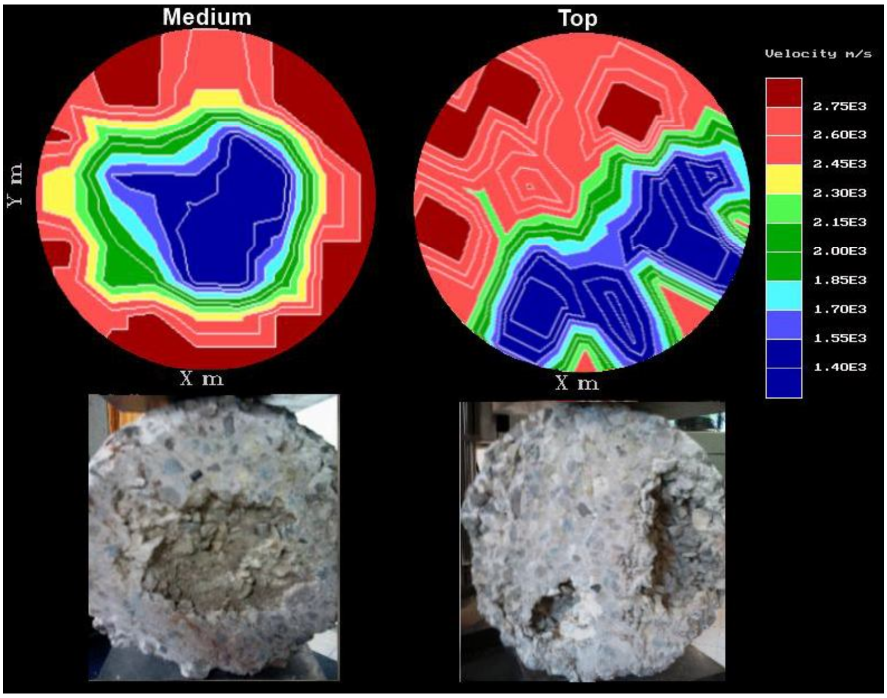

Fig. 11- Results of the ultrasonic horizontal tomography (by 3DTOM) for cylinder $C_{stone,dry}$: middle level (left above) and top level (right above). Inspection after cutting of the cylinder $Cstone_{,dry}$: middle level (left below) and top level (right below)

The highest ultrasonic velocities were generally localized in porous media with higher porosity and without fine particles, as is the case of $E_{stone,dry}$ (Fig. 13), thus revealing an effect of homogenization of the cylinder created by the grout injection. The results show a homogeneous distribution of velocities (Fig. 12 - right) which seems to indicate that the grout injection was effective. Compared to cylinder $C_{stone,dry}$ (Fig. 11) the contrast velocities are smoother and the velocity range is restricted to about 2050-2500 m/s (Fig. 12 -right). Therefore, contrary to the cylinder $C_{stone,dry}$, the cylinder $E_{stone,dry}$ presents a compact section characterized by the absence of large voids, i.e., the voids between particles of PM (before injection test) was successfully filled (Fig. 13). The results obtained by tomography were confirmed after cutting the cylinders, where it was possible to observe the aggregates connected perfectly with the grout (Fig. 12 - left), which is of the utmost importance in relation to the injection of a masonry. Indeed, it was already mentioned [52] that the reduction of the risk of failure depends highly on the degree of homogeneity of the masonry after injection. With a uniform filling the variance on the strength decreases and this way the reliability is improved.

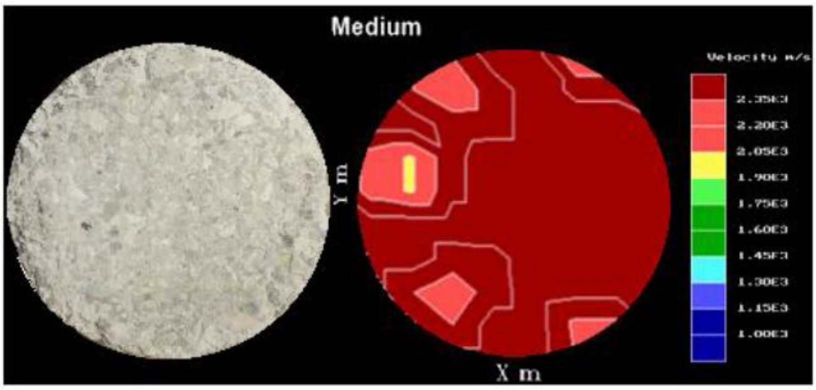

Fig. 12 - Cylinder $E_{brick,dry}$: Inspection after cutting of the cylinder (left picture) and horizontal ultrasonic tomography (by 3DTOM) (right picture)

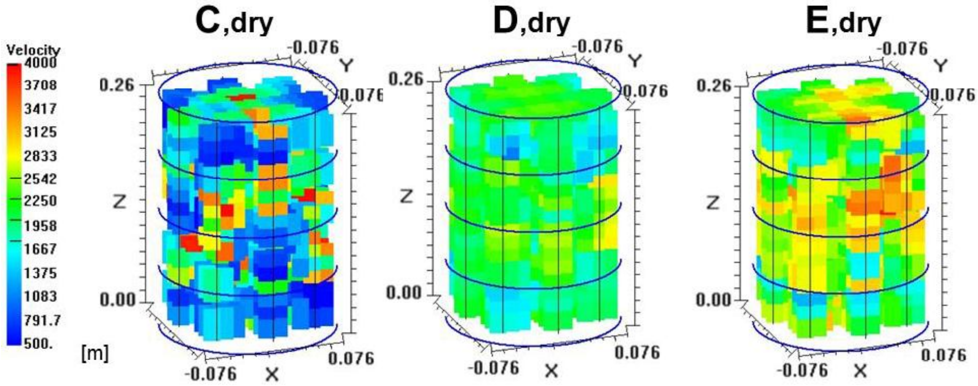

Fig. 13 - Results of the ultrasonic tomography (by GeoTom CG) - 3D tomographies for cylinders of dry limestone PM

Ultrasonic tomographies in three different levels were carried out on cylinder $C_{,brick,dry}$, as shown in Fig. 14. The tomographs show coherence with the results of Table 4 in terms of vertical distribution of the ultrasonic velocity and confirmed preliminary outcomes from visual inspection to cylinder complete (Fig. 14- lower right hand corner), which clearly indicated bad grout injection. The test with cylinder $C_{,brick,dry}$ showed that velocity decreases from bottom to top, indicating that the voids volume is significantly higher near the top level (Fig. 14). In fact, the upper horizontal tomography was characterized by smaller values of ultrasonic velocity than the lower horizontal tomography (ultrasonic velocity on the sections ranged between 900-1620 m/s and 900-2100m/s, respectively). The difference in cylinder consistency that was noted during cutting may also be detected from the comparison of the horizontal tomographs and the mechanical results along the height of the cylinder (Table 3). The tomographs displayed in Fig. 14 show, in general, that the low values of ultrasonic velocity (around 900-1200 m/s) allow the identification of areas in bad conditions, whereas areas with high velocities (higher than 1700m/s) indicate that this is a solid area of the cylinder, without voids, which shows that the voids had been successfully filled.

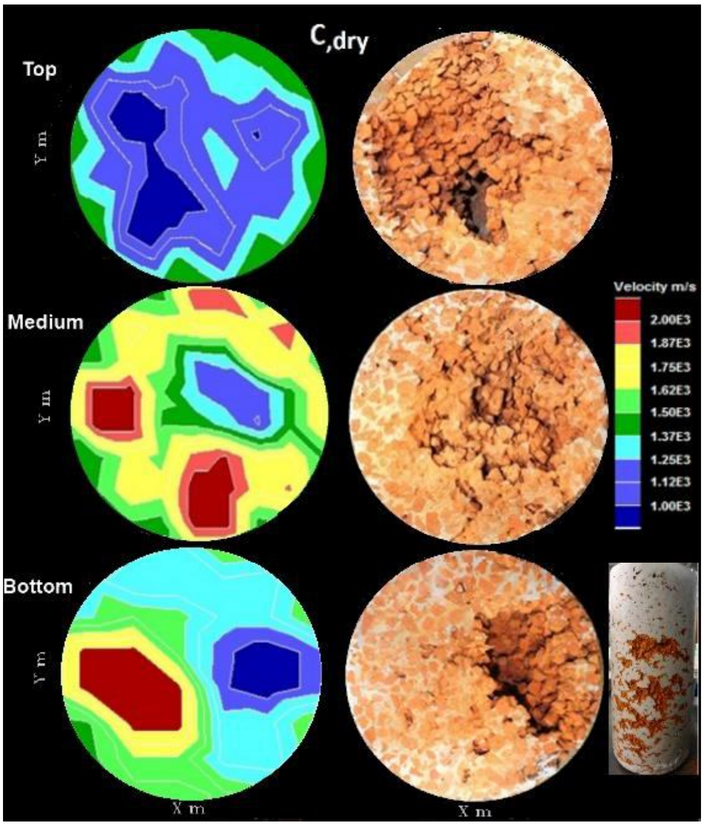

Fig. 14 - Results of the ultrasonic tomography (by 3DTOM) for cylinder $C_{brick,dry}$; horizontal tomographies, in levels: bottom, medium and top of the cylinder

As already mentioned, for the tomographs of Fig. 14, ultra sonic velocities around 900-1200 m/s correspond to areas that were not injected. The 3D tomographs from Fig. 15 confirmed the results showed previously. In fact, PM C has a considerable area along the cylinder with an ultrasonic velocity lower than 1200m/s. In contrast, in PM D and E the area is reduced. In the case of PM wetted the area is even non-existent, which proves that the voids present prior to injection were successfully filled by grout.

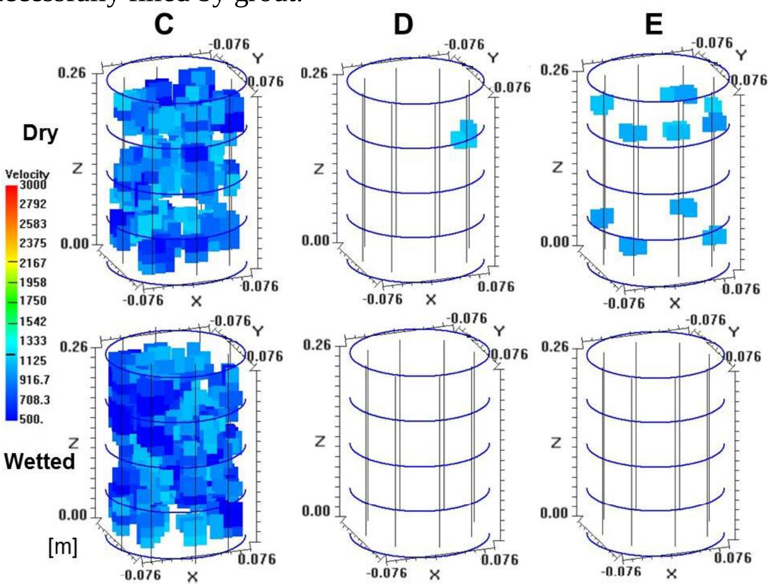

Fig. 15 - Results of the ultrasonic tomography (by GeoTom CG) - 3D tomographies (vel. < 1200 m/s) for cylinders of brick PM

Most of the applications found in the bibliography, use these results as qualitative information to assess the homogeneity and detect damage patterns of the masonry [19,53]. In this work through of the ultrasonic results it was possible to evaluate the effectiveness of grout injection depending on type of material, the particle size and water content of the porous medium at the time of grout injection.

4.5.3 Seismic resistance after grout injection

The seismic resistance of the old masonry multiple leaf walls is seriously affected due to the presence of internal voids, cracks and discontinuities between the two external leaves in a multiple leaf wall. Some of the defects of these masonry walls are poor flexibility, differential stiffness and absence of monolithic behaviour in the lateral direction which originates weak resistance to earthquake [4]. In order to attain the desired level of seismic resistance, homogeneity of the masonry is an essential principle towards strength gain. Based on the results obtained from the physical models (simulating old masonries), it can be stated that the homogeneity can be reached by injecting the grout and its effectiveness can be controlled through the ultrasonic tomography. This confirms the use of sonic tomography for in situ applications to compare the initial masonry state with the injected one and, therefore, to evaluate the improvements achieved from the seismic resistance point of view.

5 Conclusions

The main achievements attained at the present work were:

- Ultrasonic and mechanical tests showed density and strength gradients that are originated from different penetration and diffusion capacity of the grout along the injected porous medium.

- Pre-wetting process can improve the penetration of the grout inside the porous media. However, it has deleterious effects on the mechanical strength and strength gradients of the injected porous media.

- Splitting tests confirmed that the prevailing mode of failure occurs at the interface porous media particles - grout. The bond properties of the interfaces are affected by the characteristics of the particle surface and can be evaluated by the measurement of contact angle.

- For heterogeneous materials, the ultrasonic velocity depends not only on compactness but also on attenuation due to dispersion at the internal interfaces porous media particles–grout, since when a propagating wave pulse impinges on an interface, a portion of the wave energy is dissipated.

- Given the heterogeneity of the samples (porous media with different grout injections capacities) studied, the SIRT iterative method instead of RAYPT is more appropriate to perform the data inversion in the ultrasonic tomography technique. In what refers the ray tracing calculation, the curved-ray calculations are more accurate (especially for strong contrasts) to define more precisely the shape and size of the voids.

- The results of ultrasonic tomography were in accordance with visual inspections, which confirms how useful the ultrasonic tomography can be to locate non injected areas inside the cylinders that were not visually apparent, and thus to control the effectiveness of grout injection technique. Nevertheless, additional characterisation of all parameters that are attached to the tomography technique is needed, due to the complexity and variability of the process to get the tomographs. Regarding mechanical tests, it could be useful to have the information provided by shear tests (in addition to the splitting tests), since in reality this consolidation technique aims to improve the shear resistance of the masonry to be injected. In addition, the influence of the curing conditions (such as temperature and relative humidity) on the mechanical and chemical bonds between grout and porous media particles should be studied.

6 Acknowledgments

This paper is part of the research project PTDC/ECM/104376/2008, funded by FCT/MCTES, Portugal. The authors would like to acknowledge the hydraulic lime and the superplasticizers provided by Secil-Martingança and BASF-Construction Chemicals Portugal S.A, respectively, as well as to Teresa Santos and João Matos who have contributed to the preparation of materials.

7 References

[1] Uranjek M, Bosiljkov V, Zarnic R, Bokan-Bosiljkov V. *In situ tests and seismic assessment of a stone-masonry building.* s.l. : Mater Struct 2012; 45:861–879.

[2] Anzani A, Binda L, Carpinteri A, Lacidogna G, Manuello A. *Evaluation of the repair on multiple leaf stone masonry by acoustic emission* . s.l. : Mater Struct 2008; 41:1169–1189.

[3] Kalagri A, Miltiadou-Fezans A, Vintzileou E. *Design and evaluation of hydraulic lime grouts for the strengthening of stone masonry historic structures.* s.l. : Mater Struct 2010; 43:1135-1146.

[4] Chaudhry C. *Evaluation of Grouting as a Strengthening Technique for Earthen Structures in Seismic Areas: Case Study Chiripa.* s.l. : Theses (Historic Preservation), University of Pennsylvania, 2007.

[5] Luso ECP. *Análise Experimental de Caldas à Base de Cal para Injeção de Alvenaria Antiga.* s.l. : Ph.D. thesis, Universidade do Minho, 2012.

[6] Vintzileou EN, Adami, CEN. *The Bond Mechanism in Stone- or Brick-to-Grout Interfaces.* s.l. : Strain 2009; 45: 400-409.

[7] Biçer-Simsir B, Griffin I, Palazzo-Bertholon B; Rainer L. *Lime-based injection grouts for the conservation of architectural surfaces.* s.l. : Reviews in Conservation Number 10, The Getty Conservation Institute, 2009.

[8] Toumbakari EE, Van Gemert D, Tassios TP. *Methodology for the design of injection grouts for consolidation of ancient masonry.* s.l. : in "Historic Mortars: Characteristics and Tests", Internationalin RILEM Workshop 12, Paisley, Scotland, 12th-14th May 1999.

[9] Toumbakari, EE. *Lime-pozzolan-Cement grouts and their structural effects on composite masonry walls.* s.l. : Doctor Thesis, Katholieke Universiteit Leuven, 2002.

[10] Adami C, Vintzileou E. *Interventions to historic masonries: Investigation of the bond mechanism between stones or bricks and grouts.* s.l. : Mater Struct 2008; 41:255–267.

[11] Cantini L, Felicetti R, Zanzi L, Munda S, Meana M, Binda L. *Sonic Tomography applied to Historic Masonry Structures: Validation of the testing methodology and of the data elaboration by different computer codes.* s.l. : In: Proc14th International Conference – Structural Faults & Repair, 3rd–5th July 2012, Scotland [proc in cd.].

[12] Jorne F, Henriques FMA, Baltazar LG. *Grout injection in porous media with different internal structures.* s.l. : In: Proc. 14th International Conference – Structural Faults & Repair, 3rd–5th July 2012, Scotland [proc in cd.].

[13] Riggio M, Sandak A, Sandak J. *In-situ assessment of structural timber using selected wave-based NDT methods.* s.l. : Structural Analysis of Historical Constructions 2012, Wroclaw, Poland..

[14] Cantini L, Tedeschi C, Binda L, La Rosa R, Tringali S. *Non Destructive Investigation as a tool for the diagnosis of masonry damaged by the earthquake and as a support for the right choice of repair techniques.* s.l. : In: Proc14th International Conference – Structural Faults & Repair, 3rd–5th July 2012, Scotland [proc in cd.].

[15] Da Porto F, Valluzzi MR, Modena C. *Investigations for the knowledge of multi-leaf stone masonry walls.* s.l. : Proceedings of the First International Congress on Construction History, Madrid, 20th-24th January 2003.

[16] Zanzi L, Saisi A, Binda L, Cardarelli E. *Sonic Tomography of the stone pillars of a 17th century church.* s.l. : Transactions on the Built Environment vol 55, 2001.

[17] Jackson MJ, Tweeton DR. *3DTOM: Three Dimensional Geophysical Tomography.* s.l. : Reports of Investigations 9617 - U.S. Geological Survey, January 1996.

[18] Epperson GS, Abrams DP. *Non destructive evaluation of masonry buildings.* s.l. : Advanced Construction Technology Center, Doc. N. 89-26-03, October 1989, Urbana Illinois, United States, 208p.

[19] Miranda L, Rio J, Guedes J, Costa A. *Propagation of elastic waves on stone masonry walls.* s.l. : 8th International Masonry Conference 2010 in Dresden.

[20] Bras A, Henriques FMA. *Natural hydraulic lime based grouts - The selection of grout injection parameters for masonry consolidation.* s.l. : Constr. Build. Mater. 2012; 26:135–144.

[21] Jorne F, Henriques FMA, Baltazar LG. *Injection capacity of hydraulic lime grouts in different porous media.* s.l. : Mater Struct 2014; DOI: 10.1617/s11527-014-0304-9.

[22] Miltiadou-Fezans A, Tassios TP. *Penetrability of hydraulic grouts.* s.l. : Mater Struct 2013; 46:1653–1671.

[23] Valluzzi MR. *Requirements for the choice of mortar and grouts for consolidation of three-leaf stone masonry walls.* s.l. : Paper presented at the workshop repair mortars for historic masonry. Delft University of Technology, Faculty of civil Engineering and Geosciences, Delft; 26-28 January 2005.

[24] Van Rickstal F. *Grout injection of masonry, scientific approach and modeling.* s.l. : Dissertation. Katholieke Universiteit Leuven; 2000.

[25] Binda L, Anzani A. *Structural behaviour and durability of stone masonry, saving our architectural heritage: the conservation of historic stone structures.* s.l. : New York: Wiley, 1997:112-48.

[26] Almeida C, Guedes PJ, Arêde A, Costa CQ, Costa A. *Phisical characterization and compression tests of one leaf stone masonry walls.* s.l. : Constr. Build. Mater. 2012; 30:188-197.

[27] Bras A. *Grout Optmization for masonry consolidation.* s.l. : Ph.D. thesis, Faculdade de Ciências e Tecnologia da Universidade Nova de Lisboa, 2011.

[28] Eklund D, Stille H. *Penetrability due to filtration tendency of cement based grouts.* s.l. : TUNN UNDERGR SP TECH 2008; pp. 389-398.

[29] León y León, CA. *New perspectives in mercury porosimetry.* s.l. : Advances in Colloid and Interface Science 1998; 76-77:341-372.

[30] Diamond S. *Mercury porosimetry- An inappropriate method for the measurement of pore size distributions in cement-based materials.* s.l. : Cem Concr Res 2000; 30:1517-1525.

[31] Webb PA. *An Introduction to the physical characterization of materials by mercury intrusion porosimetry with emphasis on reduction and presentation of experimental data.* Norcross, Georgia : Micromeritics Instrument Corp., January 2001.

[32] Klein NS, Bachmann J, Aguado A, Toralles-Carbonari B. *Evaluation of the wettability of mortar component granular materials through contact angle measurements.* s.l. : Cem Concr Res 2012; 42:1611–1620.

[33] Pichot R, Spyropoulos F, Norton IT. *Competitive adsorption of surfactants and hydrophilic silica particles at the oil-water interface: interfacial tension and contact angle studies.* s.l. : Journal of colloid and interface science. vol. 377, no. 1, pp. 396–405, Jul. 2012.

[34] Baltazar LG, Henriques FMA, Jorne F, Cidade M. *Combined effect of superplasticizer, silica fume and temperature in the performance of natural hydraulic lime grouts.* s.l. : Constr. Build. Mater. 50: 584-597. DOI: 10.1016/j, 2014.

[35] Toumbakari EE, Van Gemert D, Tassios TP, Tenoutasse N. *Effect of mixing procedure on injectability of cimentitious grouts.* s.l. : Cem Concr Res 1999; 29:867–872.

[36] Baltazar LG, Henriques FMA, Jorne F, Cidade M. *The use of rheology in the study of the composition effects on the fresh behaviour of hydraulic lime grouts for injection of masonry walls.* s.l. : Rheol Acta 2013; 52:127–138.

[37] Baltazar LG, Henriques FMA, Jorne F. *Optimisation of flow behaviour and stability of superplasticized fresh hydraulic lime grouts through design of experiments.* s.l. : Constr Build Mater 2012, 35: 838–845.

[38] Binda L, Baronio G, Tiraboschi C, Tedeschi C. *Experimental research for the choice of adequate materials for the reconstruction of the cathedral of Noto.* s.l. : Constr Build Mater 2003; 17:629-639.

[39] Anzani A, Binda L, Lualdi M, Tedeschi C, Zanzi L. *Use of Sonic and GPR tests to control the effectiveness of grout injections of stone masonry.* s.l. : 9th European NDT Conference (ECNDT), September, 25-29, 2006 - Berlin, Germany.

[40] Moropoulou A, Labropoulos KC, Delegou, ET, Karoglou M, Bakolas A. *Non-destructive techniques as a tool for the protection of built cultural heritage.* s.l. : Constr Build Mater 2013; http://dx.doi.org/10.1016/j.conbuildmat.2013.03.044.

[41] Panzera TH, Christoforo AL, Cota FP, Borges PHR, Bowen CR. *Ultrasonic Pulse Velocity Evaluation of Cementitious Materials.* s.l. : Materials Science - Composite Materials - "Advances in Composite Materials - Analysis of Natural and Man-Made Materials", ISBN 978-953-307-449-8, Published: September 9 , 2011.

[42] Naik TR, Malhotra VM, Popovics JS. *Structural assessment and residual bearing capacity - Handbook of NDT of Concrete.* s.l. : Politecnico di Milano - Ingegneria Strutturale Corsi Felicetti, 2004.

[43] ASTM C957-02. s.l. : Standard Test Method for Pulse Velocity Through concrete, Dec 2002.

[44] Concu G, Nicolo BD, Piga C, Popescu V. *Non-Destructive Testing of Stone Masonry using Acoustic Attenuation Tomography Imaging.* s.l. : The Twelfth International Conference on Civil, Structural and Environmental Engineering Computing, Funchal - Madeira, Portugal, 1-4 September 2009, ISSN 1759-3433.

[45] Buyukozturk, O. *Imaging of concrete structures.* s.l. :NDT&E INT 1998, Vol. 31, No. 4, pp. 233-243.

[46] Schuller M, Berra M, Atkinson R, Binda L. *Acoustic Tomography for evaluation of unreinforced masonry.* s.l. : Constr Build Mater 1997, Vol.11, No.3, pp. 199-204.

[47] Concu G, De Nicolo B, Piga C, Popescu V. *Measurement System for Non-Destructive Testing using Ultrasonic Tomography Spectral Attenuation.* s.l. : 12th International Conference on Optimization of Electrical and Electronic Equipment (OPTIM), 20-22 May 2010.

[48] Ferraro CC, Boyd AJ, Consolazio GR. *Evaluation of damage to bridge piers using pulse velocity tomography.* s.l. : Constr Build Mater 2013; 38:1303–1309.

[49] Binda L, Saisi A, Tiraboschi C. *Application of sonic tests to the diagnosis of damaged and repaired structures.* s.l. : NDT&E INT 2001; 34:123-138.

[50] Axelsson M, Gustafson G, Fransson Å. *Stop mechanism for cementitious grouts at different water-to-cement ratios.* s.l. : TUNN UNDERGR SP TECH 2009; 24:390–397.

[51] Baltazar LG, Henriques FMA, Cidade M. *Performance improvement of hydraulic lime based grouts for masonry consolidation - An experimental study.* s.l. : Conf. STREMAH 2013, Southampton, UK.

[52] Van Rickstal F, Toumbakari EE, Ignoul S, Van Gemert D. *Development of mineral grouts for consolidation injection.* s.l. : In Consolidation of Masonry, Ed. D. Van Gemert, Advances in Materials Science and Restoration, 2003, pp. 61-70.

[53] Valluzzi MR, Mazzon N, Munari M, Casarin F, Modena C. *Effectiveness of injections evaluated by sonic tests on reduced scale multi-leaf masonry building subjected to seismic actions.* s.l. : NDTCE'09, Non-Destructive Testing in Civil Engineering Nantes, France, June 30th - July 3rd, 2009.